A Novel Multi-objective Protection Coordination Scheme for a Microgrid with Optimal Deployment of Dual-setting ROCOV Based Relays

Praveen Kumar Gupta, Priyanshul Niranjan, Niraj Kumar Choudhary, Nitin Singh, and Ravindra Kumar Singh

***Abstract*—Relay coordination is crucial in electrical power systems to protect against malfunctions and damage caused by unexpected events like short circuits. To address the challenge associated with the reverse direction of fault current, dual-setting (DS) directional over-current relays have evolved but failed to provide proper coordination during changes of load, generation, and network. In the meantime, with the increasing number of DS relays, the total relay operating time tends to saturate. Therefore, this paper proposes a protection scheme based on the optimal deployment of conventional and dual-setting rate of change of voltage (DS-ROCOV) relays in distribution systems. This holds true for varying network topologies and is unaffected by variations in load and generation. The objective of the proposed scheme is to ensure reliable and efficient protection against faults in distribution systems by minimizing the overall operating time with the optimal number of DS-ROCOV relays. The proposed protection scheme's performance is evaluated for different coordination time interval values as well as in different microgrid scenarios. This paper outlines the design and implementation of the proposed protection scheme which is validated on the modified IEEE 14-bus system using simulations in Matlab/Simulink.**

***Index Terms*—Coordination time interval, DS-ROCOV relay, multi-objective optimization, optimal-deployment, protection coordination.**

I. Introduction

The global emphasis on reducing carbon emissions has driven research towards the development and integration of renewable energy resources (RES), ultimately leading to the formation of microgrids (MGs) [1]. MGs are site-specific resources and range in size from a few kilowatts to megawatts based on their accessibility and location. In addition to supporting the main grid in cases of high power demand and providing appropriate power to local loads, MGs also reduce stress on transmission lines and prevent power congestion in the network [2], [3]. An MG must have an effective protection coordination scheme in order to ensure prompt, reliable, and selective relay operation to isolate the faulty parts. In comparison with unidirectional current topologies, networks with bidirectional power flows have a more complicated coordination scheme. As a result, there is a need for faster and more efficient protection schemes to cope with the situations [4].

When distributed generations (DGs) are integrated, distribution systems usually encounter a number of challenges, one of which is how it affects the protection scheme [5]. DGs influence directional over current relays (DOCRs) coordination by increasing the fault currents. As demonstrated in [6], an inverter-based DG (IBDG) has much less of an impact on protection systems than a synchronous-based DG (SBDG) due to the variance in the fault current level. The literature has discussed a number of techniques for getting the proper plug setting (PS) and time dial setting (TDS) of DOCRs to enable coordination with the least aggregate time of operation.

Trial and error techniques were initially investigated and led to a promising technique, but also encountered significant issues due to changing circumstances [7]. Another method for addressing coordination issues caused by the difference in fault current magnitudes between islanded and grid-connected operating modes is the fault current limiter (FCL). The appropriate size of FCLs has been the subject of numerous studies, but as the network topology changes, it becomes necessary to change the relay settings or the location of FCLs [8]. Nonlinear programming techniques such as genetic algorithms (GA) [9], modified firefly algorithms (MFA) [10], and gravitational search algorithms (GSA) [11],

Received: July 30, 2023
Accepted: December 18, 2023
Published Online: July 1, 2024
Praveen Kumar Gupta, Priyanshul Niranjan, Niraj Kumar Choudhary (corresponding author), Nitin Singh, and Ravindra Kumar Singh are with the Department of Electrical Engineering, Motilal Nehru National Institute of Technology Allahabad, Prayagraj 211004, India (e-mail: praveen.2021ps12@mnnit.ac.in; priyanshul.niranjan2018ree04@mnnit.ac.in; niraj@mnnit.ac.in; nitins@mnnit.ac.in; rksingh@mnnit.ac.in).
DOI:10.23919/PCMP.2023.000425

differential evolution (DE) [12], GA & grey wolf optimization (GWO) [13], etc. are utilized to obtain the optimal settings of relays. Many hybrid optimization strategies, which combine two different optimization techniques, are used to resolve the issue of trapping in local minima. Hybrid algorithms like the particle swarm optimization-gravitational search algorithm (PSO-GSA) and gravitational search algorithm-sequential quadratic programming (GSA-SQP) are investigated in [14], [15]. Additionally, references [9] and [16] examine the new generations of relays that offer user-defined time-current properties and increase the flexibility of the coordination process.

The issue of the prolong operation time of relay persists because of the bidirectional power flow. dual-setting DOCRs (DS-DOCRs) are an acceptable alternative that offers simultaneous primary and backup protection in order to address this issue. Coordination of DS-DOCRs is performed in [17]–[22] to minimize the overall operation time. Nevertheless, the method hasn't been tested across the wide range of short circuit levels under an MG's changing working conditions. As a result, whenever the operating conditions vary, it is necessary to re-adjust the PS and TDS. Also, the conventional relays are completely replaced with DS-DOCRs without considering the economic implications. As expected, the deployment of DS-DOCRs leads to a more substantial reduction in operation time, especially in the initial stages of replacement. However, the decrease in operation time reaches a saturation point as the number of DS-DOCRs increases. Hence, as demonstrated in [23], optimal deployment of the dual-setting relays is necessary to minimize the cost of the protection scheme.

Existing work falls into two categories: communication and non-communication-based approaches. While references [20]–[22] are communication-based methods, the schemes proposed in [7]–[16] do not rely on communication. As demonstrated in [20], [21], the communication system is essential to the adaptive protection schemes. It is crucial to consider the essential characteristics of communication networks, such as their cost, speed, redundancy, and dependability, prior to developing an adaptive protection scheme [22]. In addition, a communication breakdown can make a protection scheme ineffective. A multipoint technique is devised to reduce the number of violations in light of the research undertaken in [24].

A voltage-based protection approach is shown in [25], wherein the relay characteristic is determined through an extensive analysis of voltage under various fault conditions. Although the approach does not depend on operating modes, it may still operate improperly because it is extremely sensitive to even small voltage changes. In [26]–[28], a novel relay character-istic called the time-current-voltage characteristic (TCVC) is suggested. TCVC improves the operational time of an enhanced DOCR by using the fault voltage magnitude in addition to the current. The rate of change of voltage (ROCOV) has been used in several research for the detection of islanding and distance protection. The variable of ROCOV and other variables are used in [29]–[31] to accurately and quickly identify the islanding status and DG operation modes. Such an algorithm is capable of accurately distinguishing between stressed and faulty situations. As observed in [32], because of changing load and generation patterns (DG addition or removal), and changes in network topologies (line connection or disconnection, radial to mesh or vice versa), the working conditions of the system are likely to change. This in turn changes the short circuit level of the system. Because of these topological modifications, coordination time interval (CTI) violations (incoordinations) have been observed among the primary and backup over-current relays leading to healthy feeders and loads being falsely tripped. To address this problem, the ROCOV technique is applied in [33], which successfully coordinate the primary and backup relays and provides a more robust protection system regardless of the variations in generation, load, and network structure. As inferred in [34], the ROCOV relay is stable in transient situations and offers a selective, dependable, and sensitive protection mechanism without being impacted by any changes to the network topology or short circuit level. A comparative analysis of the work done in the field of MG protection is given in Table I.

TABLE I
COMPARATIVE ANALYSIS OF WORKS DONE IN THE FIELD OF MG PROTECTION

References	Year	Relay type				Operating modes		Optimization of relay characteristics	Deployment of conventional & DS relays
		DOCR	DS-DOCR	ROCOV	DS-ROCOV	Islanded mode	Grid-connected mode		
[9]	2015	√	×	×	×	×	√	√	×
[13]	2022		√	×	×	√	√	×	×
[15]	2016	√	×	×	×	×	√	×	×
[16]	2015	√	×	×	×	×	√	√	×
[17]	2020	×	√	×	×	×	√	×	×
[18]	2021	×	√	×	×	√	√	×	×
[20]	2018	×	√	×	×	√	√	×	×
[21]	2017	×	√	×	×	×	√	√	×
[23]	2019	×	√	×	×	×	√	√	√
[33]	2021	×	×	√	×	√	√	√	×
Proposed		√	√	√	√	√	√	√	√

To protect the microgrid in both islanded and grid-connected modes with constantly changing load, generation, and network topologies, this study suggests a modified protection coordination scheme for the optimal deployment of DS-ROCOV relays. The rate of change of fundamental voltage serves as the foundation for the proposed coordination scheme. The established strategy employs the built-in Matlab function "fmincon" to tackle the non-linear optimization problem. To validate the effectiveness of the proposed method, extensive numerical studies are performed. The IEEE 14-bus test system is chosen to test the performance of the proposed scheme for various fault scenarios. Furthermore, a comparative analysis with previous techniques is also performed.

The main contributions and novelties of this paper are:

1) The Pareto front and a compromise solution for the constrained multi-objective optimization problem are obtained.

2) The optimal deployment of conventional as well as DS-ROCOV relays are achieved efficiently in both grid-connected and islanded modes.

3) The impact of different CTI on the optimal deployment of relays in both operating modes of MG is observed.

4) The efficacy of the proposed protection coordination scheme with user-defined relay characteristics is tested.

5) The total operating time of relays is reduced, without violation of any relay constraints.

6) The performance of the proposed scheme for different scenarios of MG is studied.

The rest of the paper is organized as follows. An overview of DS-ROCOV relays is given in Section II. Section III addresses the problem formulation with the optimal deployment of DS-ROCOV relays, including the objective function formulation and setting up the constraints. The results and analysis for different scenarios are described in Section IV followed by a comparative analysis of the proposed scheme with different contingencies. The paper is concluded in Section V.

II. An Overview of Rocov Relays

ROCOV and relay operation time are inversely related for ROCOV-based relays, similar to that of overcurrent relays. However, the uniqueness of the proposed technique lies in the method employed to derive the "rate of voltage change". The suggested technique is based on an observation that the root-mean-square (RMS) value of fundamental voltage varies at a rate of almost zero during normal operation, but increases to greater levels in the event of a malfunction. A three-phase fault at FL1 in Fig. 1 is considered to evaluate the impact of a voltage drop brought on by a fault. The ROCOV waveforms for relay R1 during the fault, along with sinusoidal and RMS voltage waveforms, are presented in Fig. 2. A 3-phase fault is simulated between 0.2 s and 0.4 s. As can be noted, when the fault occurs (voltage decreases), the ROCOV value is negative. To verify the existence of the fault, the relay simply needs one post-fault cycle of the voltage waveform. The instantaneous fluctuation of the voltage during the transition periods is referred to as the "rate of change of voltage". Like the fault current, the value of ROCOV (R_{OCOV}) is a calculated quantity rather than a directly measured one. R_{OCOV} can be calculated using successive samples of RMS voltage at a sampling period of ΔT, as:

$$R_{\mathrm{OCOV}} = \frac{V_{(n)} - V_{(n-1)}}{\Delta T} \tag{1}$$

where $V_{(n)}$ and $V_{(n-1)}$ are the computed RMS values of phase voltage at the present sample (n) and previous sample (n-1), respectively.

As the sampling rate affects the ROCOV value, higher sampling rates (shorter sampling period) result in higher accuracy. The proposed approach, therefore, can be implemented with a sampling frequency in the range of 1–20 kHz. And in this work, a sample frequency of 20 kHz is used.

The similarity between the ROCOV curve and the standard inverse-time characteristics of DOCR is explicitly stated in [34]. As a result, the ROCOV relay's operating time (t_{op}) is inversely proportional to a function of the rate of voltage change and is described by:

$$t_{\mathrm{op}} = T^{\mathrm{DS}} \frac{A}{\left(\left| \frac{R_{\mathrm{OCOV},f}}{R_{\mathrm{OCOV,pickup}}} \right| \right)^{B} - 1} \tag{2}$$

where $R_{\mathrm{OCOV},f}$ is the rate of change of voltage during fault and $R_{\mathrm{OCOV,pickup}}$ is the pickup value of R_{OCOV}; the parameters T^{DS} (the value of TDS) and $\left|R_{\mathrm{OCOV,pickup}}\right|$ are considered as the optimization variables for standard characteristics; while the relay characteristics constants A and B are also considered variables for user-defined characteristics.

In accordance with IEC-60255, the ROCOV relay operation time is also described by time-current characteristics of the DOCR. These are classified as normal inverse (NI), very inverse (VI), and extremely inverse (EI). The associated characteristic coefficients are taken into consideration for determining each relay characteristic [17].

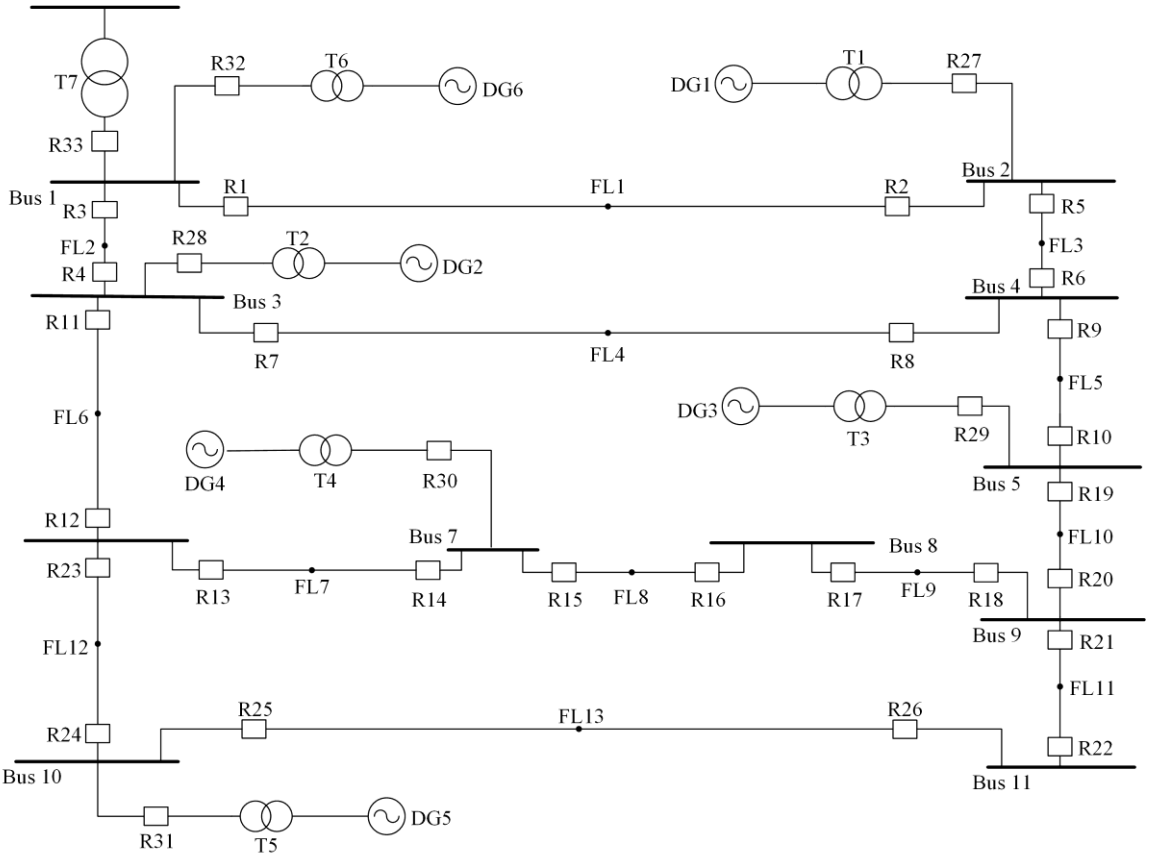

Fig. 1. Single-line diagram of the modified IEEE 14-bus system.

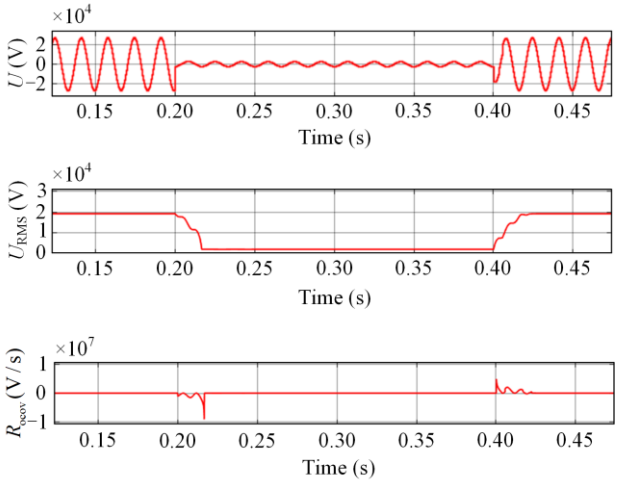

Fig. 2. Sinusoidal, RMS voltage and ROCOV waveforms for a 3-phase fault.

III. Problem Formulation with Optimal Deployment of DS-ROCOV Relays

A. Objective Function for Optimal Coordination and Deployment

The primary objective is to minimize the overall operating time of the relays that can be obtained with 100% deployment of DS-ROCOV relays. However, with the rise in the number of DS relays, the total operating time saturates. Also, the increase in the number of DS relays incurs additional costs to the protection system. Therefore, optimal deployment of DS relays is necessary to reduce the operating cost of the system as well as the total operating time. Two distinct objective functions are established to meet the requirements of the proposed coordination technique. The first one is for minimization of total relay operating time ($F^{\text{Operating\_time}}$), given by:

$$\min F^{\text{Operating\_time}} = \sum_{k\in F}\left[\sum_{i\in P}\left(t_{i,k}^{\text{fw/p}} + \sum_{j\in B_i} t_{i,k,j}^{\text{rv/b}}\right)\right] \tag{3}$$

where P, B_i and F represent the sets of the primary relay, backup relay and fault point; $t^{\text{fw/p}}$ and $t^{\text{rv/b}}$ represent the primary and backup operating times for DS-ROCOV relays; i, j and k stand for their indices. The $t^{\text{fw/p}}$ and $t^{\text{rv/b}}$ are given by:

$$t^{\text{fw/p}} = T^{\text{DSfw}} \frac{A}{\left(\left|\dfrac{R_{\text{OCOV},f}}{R_{\text{OCOV,pickup}}^{\text{fw}}}\right|\right)^{B} - 1} \tag{4}$$

$$t^{\text{rv/b}} = T^{\text{DSrv}} \frac{A}{\left(\left|\dfrac{R_{\text{OCOV},f}}{R_{\text{OCOV,pickup}}^{\text{rv}}}\right|\right)^{B} - 1} \tag{5}$$

where T^{DSfw}, $|R^{\text{fw}}_{\text{OCOV,pickup}}|$, T^{DSrv}, and $|R^{\text{rv}}_{\text{OCOV,pickup}}|$ are the four settings for the forward and reverse directions of the fault current respectively, which are the protection against fault currents in both the forward and backward directions provided by the evolution of the DS-ROCOV relay. The reverse setting of each relay is used during backup protection of the adjacent relay.

The purpose of the second objective function ($F^{\text{Dual-deployment}}$) is to determine the optimal number of DS relays as given by:

$$\min F^{\text{Dual-deployment}} = \text{Length}\ (D) \tag{6}$$

where D is the set of DS relays.

B. Coordination Constraints

Constraints play a major role in identifying the most optimal settings for effective coordination. The relays must comply with the sets of constraints given in (7), where C_{TI} is the coordination time interval required to establish discrimination between the primary and backup relays, in order to ensure the security of the proposed coordination scheme. Usually, it is restricted to the interval between 0.2 s and 0.5 s. In the proposed work C_{TI} is considered to be 0.2 s. The operation of each relay must adhere to the constraints according to its minimum ($t_{\min}$) and maximum ($t_{\max}$) operating time, i.e. 0.1 s and 2.5 s as given in (8). Along with these constraints, equations (9) and (10) illustrate how each relay's T^{DS} and $|R_{\text{OCOV,pickup}}|$ are limited by their minimum ($T^{\text{DS}}_{\min}, R_{\text{OCOV,min}}$) and maximum ($T^{\text{DS}}_{\max}, R_{\text{OCOV,max}}$) values, respectively. $|R_{\text{OCOV,pickup}}|$ is determined by the maximum rate of change of voltage during normal load switching. The minimum and maximum limits of T^{DS} are 0.05 s and 1.5 s, respectively [33]. The relay parameters A and B are additionally tuned for more flexibility in a user-defined technique. As stated in (11) and (12), A and B are guaranteed to lie between the minimum ($A_{\min}, B_{\min}$) and maximum ($A_{\max}, B_{\max}$) values i.e., (0.02, 2) and (0.14, 80), respectively.

$$t^{\text{fw/b}} - t^{\text{fw/p}},\ t^{\text{rv/b}} - t^{\text{fw/p}} \geqslant C_{\text{TI}} \tag{7}$$

$$t_{\min} \leqslant t^{\text{fw/p}},\ t^{\text{fw/b}},\ t^{\text{rv/b}} \leqslant t_{\max} \tag{8}$$

$$T^{\text{DS}}_{\min} \leqslant T^{\text{DSfw}},\ T^{\text{DSrv}} \leqslant T^{\text{DS}}_{\max} \tag{9}$$

$$R_{\text{OCOV,min}} \leqslant R^{\text{fw}}_{\text{OCOV,pickup}},\ R^{\text{rv}}_{\text{OCOV,pickup}} \leqslant R_{\text{OCOV,max}} \tag{10}$$

$$A_{\min} \leqslant A^{\text{fw}},\ A^{\text{rv}} \leqslant A_{\max} \tag{11}$$

$$B_{\min} \leqslant B^{\text{fw}},\ B^{\text{rv}} \leqslant B_{\max} \tag{12}$$

C. Optimization Technique

The coordination scheme is formulated as a non-linear constrained optimization problem. The developed optimization model is solved in Matlab using the minimum-constrained nonlinear multi-variable function (fmincon). The coordination variables are optimized for the different numbers of DS-ROCOV relays.

Since the aim is to minimize two objective functions, the most preferable solution would be the minimum value of each objective function. However, the two objectives cannot be minimized simultaneously. To find the optimal solution, a fuzzy decision-making process is used [35], [36], where each objective function is considered to have a linear membership function as represented by:

$$\mu_{i,j} = \begin{cases} 1, & F_{i,j} \leqslant F^{\min}_{i,j} \\ \dfrac{F^{\max}_{i,j} - F_{i,j}}{F^{\max}_{i,j} - F^{\min}_{i,j}}, & {}^{\min}_{i,j} \leqslant F_{i,j} \leqslant F^{\max}_{i,j} \\ 0, & F_{i,j} \geqslant F^{\max}_{i,j} \end{cases} \tag{13}$$

$$F_{i,j} = \begin{cases} F^{\text{Operating\_time}}, & \text{for } i = 1 \\ F^{\text{Dual-deployment}}, & \text{for } i = 2 \end{cases} \tag{14}$$

where $F_{i,j}$ denotes the value of ith objective function pertaining to jth Pareto-optimal solution; and the corresponding membership function $\mu_{i,j}$ assigns a degree of membership (a value between 0 and 1) to each objective function based on its importance and priority. $\mu_{i,j} = 1$ denotes the best solution ($F_{i,j} = F^{\min}_{i,j}$), and $\mu_{i,j} = 0$ denotes the worse solution ($F_{i,j} = F^{\max}_{i,j}$). The Pareto-point with highest membership value ($\mu_{i,j} = 1$) gives the best solution for individual objectives.

However, when provided with multiple objectives and a list of decision alternatives, it becomes more complex to obtain the best solution. Therefore, in the fuzzy decision-making process, a normalization step is performed on the value of each objective function ob-tained for the optimal Pareto-points. The normalization process aims to transform the objective function values into membership function values. These membership function values represent the degree to which each Pareto-optimal solution satisfies the corresponding objective function. Equation (14), which calculates the normalized membership values for both objectives, ranging from 0 to 1, is used to obtain the optimal solution. Since both objective functions $F^{\text{Operatin\_time}}$ and $F^{\text{Dual-deployment}}$ have equal importance, equal weights are assigned to them. The compromised Pareto-optimal result is eventually recognized by the membership function (μ_j) with the highest value:

$$\mu_j = \frac{\sum_{i=1}^{n} \beta_i \mu_{i,j}}{\sum_{j=1}^{m} \sum_{i=1}^{n} \beta_i \mu_{i,j}} \tag{15}$$

where β_i indicates the weight of the ith objective function; m stands for the number of Pareto-optimal solutions; and n represents the objective functions.

And Fig. 3 shows the flowchart for the proposed protection scheme.

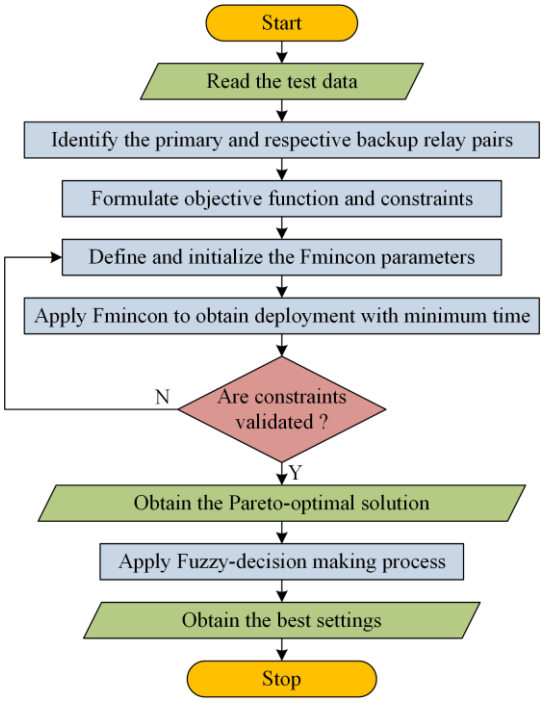

Fig. 3. Flowchart of the proposed protection scheme.

IV. Results and Analysis

The proposed strategy's efficacy is evaluated through extensive numerical studies performed on the modified IEEE 14-bus system. The test system includes 6 DGs of 6 MVA each with a grid of 200 MVA capacity. It consists of 13 lines. The system requires 32 relays in islanded mode and 33 relays in grid-connected mode for proper protection. The single-line diagram of the test system is shown in Fig. 1 and its main data are taken from [8]. The current flow in radial distribution networks is often unidirectional during faults so only one breaker is needed on the line to clear the fault. However, in meshed network configuration and network integrated with DG as shown in Fig. 1, the fault current becomes bidirectional and this needs a more complicated coordination scheme. As a result, two breakers are needed at both ends of the line to remove the fault along with a faster and more efficient protection scheme to avoid miscoordinations [16]–[18]. Under normal conditions, the MG is designed to operate in grid-connected mode, but in the case of any utility grid disruption, it seamlessly disconnects from the utility and then continues to operate in islanded mode. Therefore, optimal ROCOV relay settings are computed for both grid-connected and islanded modes.

A. Protection Scheme Based on Single-point Approach for Islanded Mode

There are 32 relays in the islanded mode of operation along with a total of 51 pairs of primary and backup relays. All of the DS-ROCOV relays are initially connected as standard relays with the optimization variables A and B as constants. Figure 4(a) displays the Pareto-optimal front obtained for the different numbers of ROCOV relays.

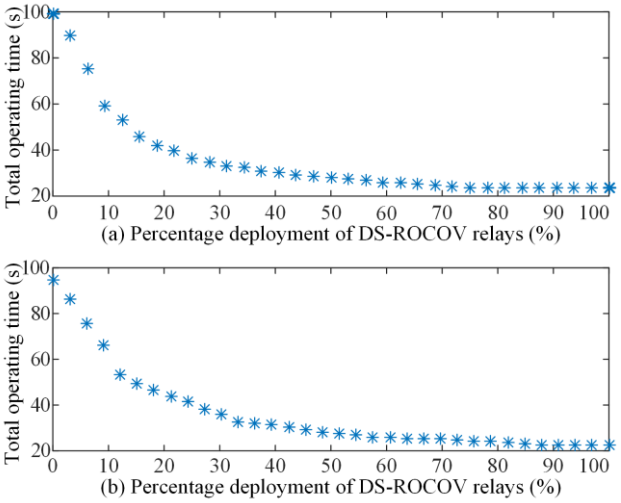

Fig. 4. Pareto-optimal front. (a) Islanded mode. (b) Grid-connected mode.

The operating times for different DS-ROCOV relay deployment percentages are shown in Table II.

TABLE II
Pareto-optimal Points for DS-ROCOV Relays Deployment in Islanded Mode

Pareto point (j)	Operating time (s)	DS-ROCOV relay (%)	μ_{1j}	μ_{2j}	μ_j
1	23.5402	100	1	0	0.0226
2	23.5402	96.875	1	0.0312	0.0233
3	23.5402	93.75	1	0.0625	0.024
4	23.5503	90.625	0.9998	0.0937	0.0247
5	23.5503	87.5	0.9998	0.125	0.0254
6	23.5503	84.375	0.9998	0.1562	0.0261
7	23.5503	81.25	0.9998	0.1875	0.0268
8	23.5503	78.125	0.9998	0.2187	0.0276
9	23.8599	75	0.9957	0.25	0.0282
10	24.1819	71.875	0.9914	0.2812	0.02887
11	24.6997	68.75	0.9846	0.3125	0.0293
12	25.2331	65.625	0.9775	0.3437	0.0299
13	25.7312	62.5	0.9709	0.375	0.0304
14	26.0799	59.375	0.9663	0.4062	0.031
15	26.8368	56.25	0.9562	0.4375	0.0315
16	27.3367	53.125	0.9496	0.4687	0.0321
17	27.8466	50	0.9429	0.5	0.0326
18	28.4332	46.875	0.9351	0.5312	0.0332
19	29.302	43.75	0.9236	0.5625	0.0336
20	30.3067	40.625	0.9102	0.5937	0.034
21	31.0768	37.5	0.9	0.625	0.0345
22	32.7273	34.375	0.8781	0.6562	0.0347
23	32.951	31.25	0.8752	0.6875	0.0354
24	34.7971	28.125	0.8507	0.7187	0.0355
25	36.6481	25	0.8262	0.75	0.0351
26	39.717	21.875	0.7855	0.7812	0.0354
27	42.0975	18.75	0.7539	0.8125	0.0354
28	46.0282	15.625	0.7018	0.8437	0.035
29	52.8744	12.5	0.611	0.875	0.0336
30	59.4411	9.375	0.5239	0.9062	0.0324
31	75.5405	6.25	0.3105	0.9375	0.0282
32	89.7604	3.125	0.1219	0.9687	0.0247
33	98.9616	0	0	1	0.0226
Best solution	34.7971	28.125	0.8507	0.7187	0.0355

The overall operating times of relays obtained with 0 and 100% deployments of DS-ROCOV relays are found to be 98.9616 s and 23.5402 s, respectively. As can be seen, using DS-ROCOV relays allows for a 77.78% reduction in overall relay operating time when compared to traditional ROCOV relays. The total operating time decreases continuously, though at a particular deployment level, the decrease in the total operating time becomes saturated. The Pareto-point that has the highest membership degree, 0.0355, produces the optimum solution, or optimal deployment percentage, of 28.125%. From Table II, it can be deduced that the operating time falls drastically from 98.9616 s to 34.7971 s for the ideal deployment of 28.125% of relays, i.e., for R1, R3, R6, R8, R10, R12, R15, R16 and R26 as DS relays. In this scenario, Tables III and IV show the obtained settings and the overall operating times at the optimal deployment. Based on the obtained settings from Table III, it is to be noted that during a fault at F1, the operating time of R1 is 0.3285 s for the forward direction and is 0.504 s for the reverse direction during a fault at F2. As a result, the forward direction relay operating time is less than that of the reverse direction. This is true for all DS relays.

TABLE III
OPTIMAL SETTINGS OF ROCOV RELAYS WITH 28.125% DEPLOYMENT LEVEL IN ISLANDED MODE

Relay	T^{DSfw} (s)	$\lvert R^{\mathrm{fw}}_{\mathrm{OCOV,pickup}} \rvert$ ($\times 10^5$ V/s)	T^{DSrv} (s)	$\lvert R^{\mathrm{rv}}_{\mathrm{OCOV,pickup}} \rvert$ ($\times 10^5$ V/s)
1	0.1504	2.3702	0.267	1.7946
2	0.1	1.2244		
3	0.1468	2.4174	0.264	1.794
4	0.1	1.2212		
5	0.1	1.2236		
6	0.1437	2.4079	0.253	2.1625
7	0.1	1.2217		
8	0.1509	2.4321	0.238	2.2827
9	0.1004	1.2455		
10	0.2178	2.4339	0.346	1.8079
11	0.1001	1.2232		
12	0.1494	2.4227	0.311	1.2537
13	0.1574	2.4239		
14	0.2203	2.4204		
15	0.1	1.2227	0.353	1.8064
16	0.1001	1.224	0.487	1.8229
17	0.3551	2.173		
18	0.1582	2.4124		
19	0.2176	2.3776		
20	0.2817	2.4304		
21	0.14	2.2989		
22	0.2741	2.4306		
23	0.1394	2.3868		
24	0.2212	2.3984		
25	0.1001	1.2271		
26	0.1001	1.2278	0.420	1.6348
27	0.2002	1.6464		
28	0.1932	1.7007		
29	0.3544	1.7304		
30	0.3622	1.6504		
31	0.3764	1.3667		
32	0.2761	1.5926		

TABLE IV
RELAY OPERATING TIME WITH 28.125 % DEPLOYMENT LEVEL IN ISLANDED MODE

Fault location	Primary (s)	Backup (s)		
FL1	R1	R3	R32	
	0.3285	0.5294	0.5325	
	R2	R6	R27	
	0.1779	0.3782	0.3873	
FL2	R3	R1	R32	
	0.3032	0.504	0.5036	
	R4	R8	R12	R28
	0.1813	0.3814	0.3984	0.3859
FL3	R5	R1	R27	
	0.1712	0.3715	0.3716	
	R6	R8	R10	
	0.3182	0.5186	0.5487	
FL4	R7	R12	R28	R3
	0.1782	0.3784	0.3786	0.3807
	R8	R6	R10	
	0.3229	0.5233	0.523	
FL5	R9	R6	R8	
	0.1634	0.4795	0.4573	
	R10	R20	R29	
	0.4196	0.6197	0.6201	
FL6	R11	R3	R28	R8
	0.1802	0.3804	0.3829	0.401
	R12	R14	R24	
	0.3149	0.5151	0.537	
FL7	R13	R12	R24	
	0.3082	0.5086	0.5084	
	R14	R30	R15	
	0.4195	0.6199	0.6204	
FL8	R15	R13	R30	
	0.1624	0.3626	0.6361	
	R16	R18		
	0.1579	0.3581		
FL9	R17	R16		
	0.6497	0.8506		
	R18	R19	R22	
	0.3114	0.5117	0.6132	
FL10	R19	R10	R29	
	0.4254	0.6263	0.6326	
	R20	R17	R22	
	0.5369	0.7371	0.7371	
FL11	R21	R17	R19	
	0.3131	0.8403	0.5667	
	R22	R26		
	0.5404	0.7408		
FL12	R23	R12	R14	
	0.3112	0.5701	0.5418	
	R24	R31	R26	
	0.4462	0.6465	0.7588	
FL13	R25	R31	R23	
	0.177	0.6856	0.3775	
	R26	R21		
	0.1687	0.3691		

B. Protection Scheme Based on Single-point Approach for Grid-connected Mode

When connected to the grid the total number of primary and backup relay pairs increases to 53 with the addition of one more relay on the grid side. Figure 4(b) displays the Pareto-optimal front. The operating times for various DS-ROCOV relay deployment percentages are shown in Table V.

TABLE V
PARETO-OPTIMAL POINTS FOR DS-ROCOV RELAYS DEPLOYMENT IN GRID-CONNECTED MODE

Pareto point (j)	Operating time (s)	DS-ROCOV relay (%)	μ_{1j}	μ_{2j}	μ_j
1	22.5934	100	1	0	0.0223
2	22.5934	96.9697	1	0.0303	0.0229
3	22.5934	93.9394	1	0.0606	0.0236
4	22.5934	90.9091	1	0.0909	0.0243
5	22.6089	87.8788	1	0.1212	0.025
6	23.1275	84.8485	1	0.1515	0.0256
7	23.7998	81.8182	0.9964	0.1818	0.0262
8	23.9195	78.7879	0.9947	0.2121	0.0269
9	24.4768	75.7576	0.9869	0.2424	0.0274
10	24.1291	72.7273	0.9909	0.2727	0.0281
11	25.1847	69.697	0.9778	0.303	0.0285
12	25.2611	66.6667	0.9745	0.3333	0.0291
13	25.3627	63.6364	0.9759	0.3636	0.0298
14	25.8272	60.6061	0.9664	0.3939	0.0303
15	25. 9387	57.5758	0.968	0.4242	0.031
16	27.147	54.5455	0.9466	0.4545	0.0312
17	27. 3569	51.5152	0.9495	0.4848	0.0319
18	28.1346	48.4848	0.9357	0.5152	0.0323
19	29.0724	45.4545	0.9225	0.5455	0.0327
20	30.189	42.4242	0.9069	0.5758	0.033
21	31.5654	39.3939	0.8876	0.6061	0.0333
22	31.7573	36.3636	0.8849	0.6364	0.0339
23	32.7433	33.3333	0.8711	0.6667	0.0342
24	35.7697	30.303	0.8287	0.697	0.034
25	37.9545	27.2727	0.7982	0.7273	0.034
26	41.4825	24.2424	0.7487	0.7576	0.0335
27	43.7124	21.2121	0.7175	0.7879	0.0335
28	46.7538	18.1818	0.6749	0.8182	0.0332
29	49.6054	15.1515	0.635	0.8485	0.033
30	53.1642	12.1212	0.5852	0.8788	0.0326
31	66.4228	9.0909	0.3995	0.9091	0.0291
32	75.7769	6.0606	0.2685	0.9394	0.0269
33	86.532	3.0303	0.1179	0.9697	0.0242
34	94.9524	0	0	1	0.0223
Best solution	32.7433	33.3333	0.8711	0.6667	0.0342

The overall operating times of relays obtained with 0 and 100% deployment of DS-ROCOV relays are found to be 94.9524 s and 22.5934 s, respectively. As can be seen, using DS-ROCOV relays allows a 75.41% reduction in the overall relay operation time which is the same as in the islanded mode of operation. The Pareto-point that has the highest membership degree, 0.0342, provides the optimum solution with 33.3333% DS-ROCOV relays. From Table VI, it can be inferred that for the ideal deployment of 33.33% of relays, i.e., for R3, R6, R8, R9, R12, R14, R17, R18, R20, R24 and R26 working as DS relays, operating time substantially decreases from 94.9524 s to 32.7433 s. In this scenario, Table VII shows the overall operating times at the optimal deployment. The operating times of relay R3 in forward and reverse directions during a fault at FL2 and FL1 are 0.2887 s and 0.4975 s, respectively. As can be seen, the relay operates in a shorter period in the forward direction than in the reverse direction in grid-connected mode. This is similar to islanded mode.

TABLE VI
OPTIMAL SETTINGS OF ROCOV RELAYS WITH 33.33% DEPLOYMENT LEVEL IN GRID-CAONNECTED MODE

Relay	T^{DSfw} (s)	$\lvert R^{\mathrm{fw}}_{\mathrm{OCOV,pickup}} \rvert$ ($\times 10^5$ V/s)	T^{DSrv} (s)	$\lvert R^{\mathrm{rv}}_{\mathrm{OCOV,pickup}} \rvert$ ($\times 10^5$ V/s)
1	0.1221	1.9971		
2	0.1928	1.9982		
3	0.119	1.9983	0.228	1.4586
4	0.085	1.0005		
5	0.085	1.0006		
6	0.2396	1.9964	0.265	1.3473
7	0.085	1.0003		
8	0.1617	1.3566	0.329	1.9897
9	0.1378	1.9829	0.350	1.65
10	0.085	1.0005		
11	0.085	1.0004		
12	0.1424	1.9984	0.207	1.0071
13	0.085	1.0017		
14	0.2144	1.9971	0.272	1.4735
15	0.1471	1.9834		
16	0.2783	1.9882		
17	0.085	1.0016	0.417	1.4853
18	0.0851	1.0054	0.311	1.0036
19	0.085	1.0018		
20	0.1527	1.9962	0.214	1.9845
21	0.1273	1.9909		
22	0.2212	1.9896		
23	0.0851	1.0047		
24	0.2076	1.9949	0.179	1.4553
25	0.0851	1.0024		
26	0.085	1.0011	0.360	1.3663
27	0.34	1.1385		
28	0.1973	1.0158		
29	0.1995	1.3145		
30	0.3643	1.2635		
31	0.3717	1.0207		
32	0.2272	1.4742		
33	0.2272	1.4742		

TABLE VII
RELAY OPERATING TIME WITH 33.33% DEPLOYMENT LEVEL IN GRID-CONNECTED MODE

Fault location	Primary (s)	Backup (s)			Fault location	Primary (s)	Backup (s)	
FL1	R1	R3	R32	R33	FL8	R15	R14	R30
	0.2974	0.4975	0.4974	0.4974		0.2846	0.4848	0.6217
	R2	R6	R27			R16	R17	
	0.4061	0.6061	0.6061			0.5199	0.7201	
FL2	R3	R2	R32	R33	FL9	R17	R15	
	0.2887	0.4887	0.4957	0.4957		0.1313	0.3313	
	R4	R8	R12	R28		R18	R20	R22
	0.1503	0.3504	0.3593	0.3503		0.1388	0.421	0.4958
FL3	R5	R1	R27		FL10	R19	R9	R29
	0.1534	0.3534	0.6361			0.1334	0.3395	0.3511
	R6	R8	R9			R20	R18	R22
	0.5371	0.7372	0.7372			0.2848	0.4849	0.4849
FL4	R7	R12	R28	R3	FL11	R21	R18	R20
	0.158	0.358	0.3683	0.3758		0.2947	0.5806	0.4947
	R8	R6	R9			R22	R26	
	0.3125	0.5126	0.7187			0.4279	0.628	
FL5	R9	R6	R8		FL12	R23	R12	R14
	0.2775	0.4779	0.6637			0.1581	0.3855	0.533
	R10	R20	R29			R24	R31	R26
	0.1323	0.3323	0.3324			0.4109	0.6109	0.6407
FL6	R11	R3	R28	R8	FL13	R25	R31	R24
	0.1621	0.3621	0.3778	0.4078		0.1492	0.6553	0.3494
	R12	R14	R24			R26	R21	
	0.294	0.494	0.494			0.143	0.3431	
FL7	R13	R12	R24					
	0.1386	0.3387	0.4769					
	R14	R30	R16					
	0.3988	0.5989	0.5989					

C. Protection Scheme with Different CTI Values

Typically, C_{TI}, i.e., CTI values, lies in the range of 0.2 s to 0.5 s. Based on this, optimal deployment percentages and respective operating times for different C_{TI} values in islanded mode is shown in Table VIII, and Table IX shows optimal deployment percentages and respective operating times for different CTI values in grid-connected mode. It can be seen that, to large extent, the ideal solution (i.e., percentage deployment) does not vary for different CTIs. This is because the ROCOV relay time characteristics are parallel inverse curves that indicate various time dial settings, and thus the difference between the curves stays rather constant throughout a range of CTI values, so the optimal deployment percentage remains the same, i.e., 28.125% in islanded mode and 33.33% in grid-connected mode. Nevertheless, under the same optimal deployment percentage, the overall time of operation increases with an increase in the CTI values. This is attributed to the fact that in order to maintain proper coordination with the primary relays, the backup relays have to exhibit an operating time much higher than the primary relays. Besides, Table VIII and Table IX show that for CTI values of 0.2 s, 0.3 s, and 0.4 s, respectively, the overall operating times are 34.7971 s, 55.1202 s, and 66.1223 s in islanded mode, and 32.7433 s, 47.0143 s, and 56.8997 s in grid-connected mode.

TABLE VIII
SIMULATION RESULTS FOR DIFFERENT CTI VALUES IN ISLANDED MODE

Pareto-Point (j)	DS-ROCOV (%)	Operating time (s)		μ_j	
		$C_{TI}=0.3$	$C_{TI}=0.4$	$C_{TI}=0.3$	$C_{TI}=0.4$
1	100	28.8339	33.959	0.0231	0.0235
2	96.875	28.8339	33.959	0.0238	0.0243
3	93.75	28.8339	33.959	0.0245	0.025
4	90.625	28.8339	33.959	0.0253	0.0257
5	87.5	29.6744	33.959	0.0258	0.0265
6	84.375	30.1435	34.6211	0.0264	0.0271
7	81.25	30.1716	37.032	0.0272	0.0273
8	78.125	31.2847	37.1902	0.0277	0.028
9	75	32.0962	37.3073	0.0282	0.0287
10	71.875	32.4402	37.504	0.0289	0.0294
11	68.75	34.1477	40.233	0.0293	0.0296
12	65.625	33.4521	40.1925	0.0301	0.0304
13	62.5	34.868	40.5302	0.0306	0.0311
14	59.375	34.8134	42.9624	0.0313	0.0313
15	56.25	35.5387	43.9946	0.0319	0.0318
16	53.125	36.3874	44.8047	0.0325	0.0324
17	50	39.1468	45.3077	0.0326	0.0331
18	46.875	38.8233	49.0311	0.0334	0.0331
19	43.75	40.7232	48.2649	0.0351	0.034
20	40.625	42.655	54.475	0.0341	0.0335
21	37.5	43.6044	54.085	0.0347	0.0343
22	34.375	47.4944	60.1926	0.0346	0.0338
23	31.25	49.949	60.8663	0.0349	0.0342
24	28.125	55.1202	66.1223	0.0361	0.0344
25	25	56.6613	70.171	0.035	0.0341
26	21.875	57.2639	74.819	0.0356	0.0339
27	18.75	69.2089	78.5906	0.034	0.0339
28	15.625	71.8233	91.108	0.0343	0.0322
29	12.5	83.4345	100.428	0.0327	0.0311
30	9.375	102.718	101.021	0.0297	0.0317
31	6.25	111.404	116.624	0.0288	0.0294
32	3.125	133.745	129.528	0.0252	0.0276
33	0	148.248	154.356	0.0231	0.0235
Best solution	28.125	55.1202	66.1223	0.0361	0.0344

TABLE IX
SIMULATION RESULTS FOR DIFFERENT CTI VALUES IN GRID-CONNECTED MODE

Pareto-point (*j*)	DS-ROCOV (%)	Operating time (s)		μ_j	
		$C_{\text{TI}}=0.3$	$C_{\text{TI}}=0.4$	$C_{\text{TI}}=0.3$	$C_{\text{TI}}=0.4$
1	100	28.0385	33.4981	0.0226	0.0223
2	96.9697	28.0385	33.4981	0.0233	0.0229
3	93.9394	28.0385	33.4981	0.024	0.0236
4	90.9091	28.5008	33.4981	0.0246	0.0243
5	87.8788	28.5008	34.728	0.0253	0.025
6	84.8485	29.1195	35.0932	0.0258	0.0256
7	81.8182	30.0462	36.5141	0.0263	0.0262
8	78.7879	30.2979	35.9699	0.0269	0.0269
9	75.7576	31.1875	38.6806	0.0275	0.0274
10	72.7273	31.9009	38.8705	0.028	0.0281
11	69.697	31.1839	37.4971	0.0288	0.0285
12	66.6667	31.291	39.114	0.0295	0.0291
13	63.6364	33.6167	39.934	0.0297	0.0298
14	60.6061	34.2382	41.8661	0.0303	0.0303
15	57.5758	34.1289	42.2786	0.031	0.031
16	54.5455	36.6482	43.2225	0.0312	0.0312
17	51.5152	35.7807	44.3781	0.032	0.0319
18	48.4848	36.4801	47.1569	0.0326	0.0323
19	45.4545	39.6074	50.001	0.0326	0.0327
20	42.4242	40.8137	53.1164	0.0331	0.033
21	39.3939	43.1644	53.3811	0.0333	0.0333
22	36.3636	43.1761	52.9607	0.034	0.0339
23	33.3333	47.0143	56.8997	0.0341	0.0342
24	30.303	52.1757	67.5392	0.0336	0.034
25	27.2727	52.7819	68.2385	0.034	0.034
26	24.2424	57.2981	72.2268	0.0339	0.0335
27	21.2121	65.2086	75.5776	0.0331	0.0335
28	18.1818	69.9659	88.7945	0.0328	0.0332
29	15.1515	79.1209	92.0987	0.0317	0.033
30	12.1212	84.5626	104.471	0.0313	0.0326
31	9.0909	99.4886	118.862	0.029	0.0291
32	6.0606	112.097	134.758	0.0272	0.0269
33	3.0303	129.063	146.394	0.0245	0.0242
34	0	142.225	158.380	0.0226	0.0223
Bestsolution	33.33333	47.0143	56.8997	0.0341	0.0342

D. Protection Scheme Based on User-defined characteristics.

For greater adaptability, the user-defined coordination approach is preferred where coefficients A and B are also included in the optimization process along with T^{DS} and $|R_{\text{OCOV,pickup}}|$. The optimization procedure in this scenario includes eight variables for DS-ROCOV relays and four variables for conventional ROCOV relays. Table X and Table XI show that the relay settings which are well optimized using the proposed protection mechanism, while Table XII and Table XIII show that the operating times for different fault locations for both the grid-connected mode and the islanded mode of operation, respectively. The results show that with the optimized four settings, it is possible to reduce the overall operating time for the relays while retaining relay coordination. At the optimal deployment percentage found in part A and part B of Section IV, the overall operating times for islanded mode and grid-connected mode by using this protection scheme are 30.5664 s and 26.1276 s respectively, which are earlier compared to previous 34.7971 s and 32.7433 s. There are reductions in total operating times, so it can be concluded that user-defined characteristics provide a more flexible, efficient, and fast protection scheme.

TABLE X
OPTIMAL SETTINGS OF USER-DEFINED ROCOV RELAYS WITH 33.33 % DEPLOYMENT LEVEL IN GRID-CONNECTED MODE

Relay	T^{DSfw}	$\lvert R^{\text{fw}}_{\text{OCOV,pickup}}\rvert$	T^{DSrv}	$\lvert R^{\text{rv}}_{\text{OCOV,pickup}}\rvert$	A^{fw}	B^{fw}	A^{rv}	B^{rv}
1	0.94	1.82			2.6	0.8		
2	0.94	1.77			2.5	0.7		
3	1.04	1.93	0.69	1.51	3.3	1	1.9	0.4
4	0.36	1.44			1.9	0.6		
5	0.97	1.8	0.71	1.53	2.9	0.9	2	0.4
6	0.41	1.45			2	0.7		
7	0.41	1.46	0.62	1.47	1.8	0.6	2	0.5
8	0.41	1.46	0.69	1.52	2	0.7	2.1	0.5
9	0.41	1.43			1.9	0.6		
10	1.05	1.89	0.73	1.54	3.3	0.9	2.1	0.4
11	1.1	1.96	0.7	1.52	3.6	1.1	2.1	0.5
12	0.35	1.42			1.9	0.6		
13	0.41	1.43			1.9	0.6		
14	0.94	1.72	0.66	1.53	2.5	0.7	2	0.4
15	0.7	1.59	0.72	1.55	2.2	0.6	2.2	0.4
16	0.39	1.42			1.9	0.5		
17	0.44	1.44	0.64	1.52	2	0.6	2	0.4
18	0.4	1.43	0.52	1.43	1.8	0.6	1.9	0.3
19	0.96	1.74			2.6	0.7		
20	0.96	1.78			2.7	0.7		
21	0.78	1.67			2.4	0.7		
22	0.83	1.63			2.2	0.5		
23	1.05	1.9			3.2	1		
24	0.87	1.67			2.5	0.7		
25	1	1.59			2.1	0.9		
26	0.51	1.46	0.69	1.52	2	0.7	2.1	0.3
27	0.67	1.5			2	0.4		
28	0.75	1.54			2.4	0.5		
29	0.69	1.52			2	0.4		
30	0.7	1.52			2.1	0.4		
31	0.64	1.49			2	0.4		
32	0.72	1.52			2.1	0.5		
33	0.72	1.52			2.1	0.5		

TABLE XI
OPTIMAL SETTTINGS OF USER-DEFINED ROCOV RELAYS WITH 28.125 % DEPLOYMENT LEVEL IN ISLANDED MODE

Relay	T^{DSfw}	$\lvert R^{fw}_{OCOV,pickup} \rvert$	T^{DSrv}	$\lvert R^{rv}_{OCOV,pickup} \rvert$	A^{fw}	B^{fw}	A^{rv}	B^{rv}
1	0.97	2.08			1.5	0.5		
2	1.03	2.26			1.8	0.6		
3	1.06	2.43	0.91	1.88	2.5	0.8	1.3	0.3
4	0.72	1.79			1.2	0.7		
5	1.04	2.27			1.9	0.6		
6	1.04	2.31			1.6	0.5		
7	0.73	1.8			1.3	0.7		
8	1.03	2.25	0.94	1.93	2.2	0.7	1.5	0.4
9	1.05	2.29			2	0.6		
10	1.06	2.43			2.1	0.6		
11	1.06	2.39			2.9	0.9		
12	1.05	2.3			2	0.8		
13	0.73	1.8			1.3	0.6		
14	1.04	2.21	0.9	1.89	1.9	0.6	1.4	0.4
15	0.86	1.93			1.4	0.5		
16	0.96	1.99			1.5	0.4		
17	0.74	1.81	0.98	1.96	1.3	0.6	1.6	0.3
18	0.69	1.79	0.84	1.79	1.2	0.6	1.3	0.3
19	1.06	2.44			2.6	0.8		
20	1.04	2.23			1.9	0.5		
21	1.03	2.25	0.9	1.87	2	0.8	1.3	0.3
22	0.69	1.79			1.2	0.6		
23	1.04	2.43			2.5	0.9		
24	1.02	2.13			1.7	0.6		
25	0.75	1.82			1.3	0.7		
26	0.72	1.81	0.94	1.91	1.3	0.6	1.4	0.4
27	0.94	1.91	0.72	1.81	1.5	0.4	1.3	1
28	0.98	1.97			1.7	0.5		
29	0.94	1.9			1.5	0.3		
30	0.94	1.9	0.72	1.81	1.4	0.4	1.3	1
31	0.91	1.88			1.4	0.4		
32	0.93	1.9			1.4	0.3		

TABLE XII
RELAY OPERATING TIME WITH 33.33% DEPLOYMENT LEVEL IN GRID-CONNECTED MODE

Fault location	Primary (s)	Backup (s)		
FL1	R1	R3	R32	R33
	0.27	0.5047	0.4868	0.4868
	R2	R5	R27	
	0.291	0.529	0.5003	
FL2	R3	R2	R32	R33
	0.2255	0.4364	0.4836	0.4836
	R4	R7	R11	R28
	0.1	0.3074	0.3212	0.3526
FL3	R5	R1	R27	
	0.1931	0.3999	0.5469	
	R6	R8	R10	
	0.102	0.3812	0.317	
FL4	R7	R11	R28	R3
	0.1063	0.3591	0.3956	0.4462
	R8	R5	R10	
	0.1	0.3001	0.2886	
FL5	R9	R5	R8	
	0.1	0.3005	0.315	
	R10	R20	R29	
	0.1388	0.3398	0.3965	
FL6	R11	R3	R28	R7
	0.2047	0.4083	0.4189	0.4749
	R12	R14	R24	
	0.1	0.3341	0.3287	
FL7	R13	R11	R24	
	0.1	0.3122	0.3046	
	R14	R30	R15	
	0.2016	0.4302	0.4469	
FL8	R15	R14	R30	
	0.2287	0.4643	0.4619	
	R16	R17		
	0.1048	0.3474		
FL9	R17	R15		
	0.1011	0.3111		
	R18	R19	R22	
	0.1058	0.3532	0.4628	
FL10	R19	R10	R29	
	0.2159	0.4584	0.4401	
	R20	R18	R22	
	0.2347	0.4374	0.4442	
FL11	R21	R18	R19	
	0.2176	0.5965	0.4224	
	R22	R26		
	0.349	0.5609		
FL12	R23	R11	R14	
	0.1805	0.3736	0.393	
	R24	R31	R26	
	0.2161	0.429	0.5809	
FL13	R25	R31	R23	
	0.1	0.4908	0.29	
	R26	R21		
	0.1008	0.3038		

TABLE XIII
RELAY OPERATING TIME WITH 28.125 % DEPLOYMENT LEVEL IN ISLANDED MODE

Fault location	Primary (s)	Backup (s)		
FL1	R1	R3	R32	
	0.4513	0.6695	0.6607	
	R2	R6	R27	
	0.3477	0.5509	0.6061	
FL2	R3	R2	R32	
	0.2311	0.4368	0.6017	
	R4	R8	R12	R28
	0.1084	0.3714	0.34	0.4212
FL3	R5	R1	R27	
	0.3522	0.5566	0.564	
	R6	R8	R10	
	0.3993	0.616	0.6007	
FL4	R7	R12	R28	R3
	0.1017	0.3032	0.4052	0.405
	R8	R5	R10	
	0.2541	0.3001	0.2886	
FL5	R9	R5	R8	
	0.2739	0.4778	0.5027	
	R10	R20	R29	
	0.3437	0.5498	0.5545	
FL6	R11	R3	R28	R8
	0.2006	0.4043	0.4147	0.4129
	R12	R14	R24	
	0.1948	0.3992	0.3997	
FL7	R13	R11	R24	
	0.1056	0.3074	0.359	
	R14	R30	R16	
	0.2562	0.4697	0.4643	
FL8	R15	R14	R30	
	0.2422	0.4644	0.4921	
	R16	R17		
	0.3756	0.5996		
FL9	R17	R15		
	0.1051	0.3121		
	R18	R19	R21	
	0.1075	0.3176	0.6564	
FL10	R19	R9	R29	
	0.1944	0.4	0.5738	
	R20	R18	R21	
	0.4178	0.6232	0.6244	
FL11	R21	R18	R19	
	0.2066	0.7945	0.4061	
	R22	R26		
	0.114	0.4642		
FL12	R23	R11	R14	
	0.1808	0.3758	0.4415	
	R24	R31	R26	
	0.2738	0.4841	0.4851	
FL13	R25	R31	R23	
	0.1019	0.5398	0.3013	
	R26	R21		
	0.1028	0.3061		

E. Comparative Analysis of the Proposed Scheme.

In Fig. 5, the performance of DS-ROCOV and DS-DOCR is compared in terms of the overall relay operating time. For islanded and grid-connected modes, the overall operating time at optimal deployment is 37.1661 s and 34.7702 s for DS-DOCR, and 34.7702 s and 32.7433 s for DS-ROCOV relay, respectively. Even at the 0 and 100% deployment levels, the relay operating times for DS-ROCOV relay are shorter than DS-DOCR in both operating modes. In respective islanded and grid-connected modes at 0% deployment, the operating times are 102.2233 s and 97.7445 s forThe DS-DOCR, and 98.9616 s and 94.9524 s for the DS-ROCOV relay. At 100% deployment, the respective operating times are 31.7617 s and 29.4398 s for the DS-DOCR, and 23.5402 s and 22.5934 s for the DS-ROCOV relay.

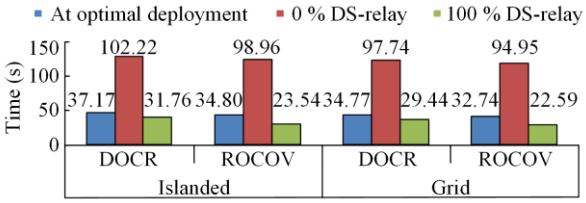

Fig. 5. Operating time at different deployment level.

The comparisons between the primary and backup relay operating times for the DS-DOCR and DS-ROCOV relays in both islanded and grid-connected modes are shown in Figs. 6 and 7, respectively. Compared to DS-DOCR, it can be seen that some DS-ROCOV relays (working either as primary or backup) have higher operating times in both islanded and grid-connected modes, though the total operating time is less for DS-ROCOV relays. For all the investigated fault locations, the results shown in Fig. 8 compare the computed C_{TI} using DS-DOCR and DS-ROCOV relays for 53 primary-backup pairs. The minimum and maximum C_{TI} obtained are 0.2 s and 0.3136 s for the DS-DOCR, and 0.2s and 0.5272 s for DS-ROCOV relays.

It is evident that both DS-DOCR and DS-ROCOV satisfy the CTI constraint in normal working conditions. However, the working condition of the system can change. Therefore a performance analysis of the pro-posed scheme is carried out for different scenarios in both islanded and grid-connected modes for all 13 fault locations.

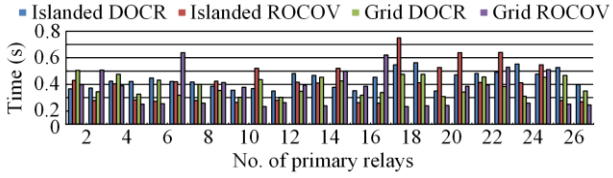

Fig. 6. Primary relay operating time for both operating modes.

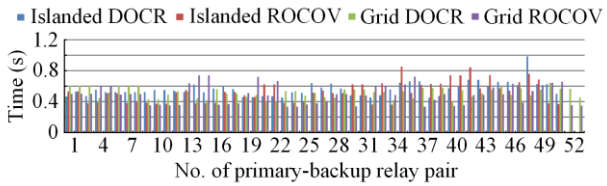

Fig. 7. Backup relay operating time for both operating modes.

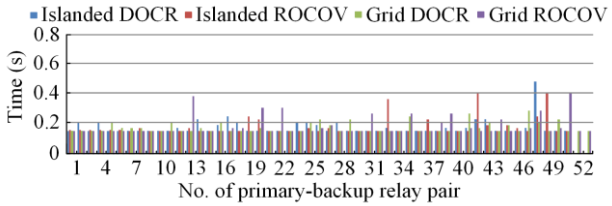

Fig. 8. CTI for both operating modes.

Because changing loads and generation, the working conditions of the system change. This in turn changes the short circuit level of the system. This can cause the overall system reliability to decrease, and conventional DOCRs can no longer achieve proper coordination. Any protection schemes that violate the constraints related to the relay coordination problem are no longer effective. However, proper coordination can be achieved using ROCOV relays as they are not affected by the changing short circuit levels. Tables XIV and XV describe the different examined scenarios and the number of miscoordinations occurring with DS-DOCR and DS-ROCOV relays.

TABLE XIV
LIST OF DIFFERENT SCENARIOS EXAMINED

Scenario	State
1	Disconnecting DGs in grid-connected mode
2	Adding extra DGs to increase short circuit level in grid-connected mode
3	Adding extra DGs to increase short circuit level in islanded mode

TABLE XV
COORDINATION CONSTRAINT VIOLATION SUMMARY

Scenario	Bus No. (DG conect/disconnect)	Constraint violation in DS-DOCR	Constraint violation in DS-ROCOV
1	2	5	0
	3	6	0
	1 & 10	10	0
	1, 3 & 7	11	0
2	4	10	0
	6 & 11	8	0
3	4	19	0
	6 & 11	18	0

In scenario 1, the effect of reducing the short circuit level by disconnecting single and multiple DGs is examined. As is seen from Table XV, number 5 and 6 of DS-DOCRs fail to maintain the coordination of the protection system (i.e., C_{TI} is less than 0.2 s) when the DGs situated at buses 2 and 3 are disconnected, respectively. In certain scenarios with DS-DOCRs, there are instances where the backup relay operates in a shorter period of time than the primary relay. This can lead to the backup DOCR taking precedence over the primary DOCR, resulting in a negative C_{TI}. When two DGs are disconnected at buses 1 and 10, there are 10 C_{TI} violations, whereas 11 relays violate the C_{TI} constraint when three DGs are disconnected at buses 1, 3 and 7, respectively. However, in all cases of DG disconnection, no C_{TI} violation is found for DS-ROCOV relays. In scenarios 2 and 3, the effects of increasing short-circuit levels in grid-connected and islanded modes are investigated, respectively. Additional DGs are added to the network in both operating modes to raise the total short circuit level, while the added DGs are of the same rating as those used in the test system [8]. It can be deduced from Table XV that a number of miscoordinations are observed using DS-DOCRs whereas the C_{TI} for all fault locations based on ROCOV relays are above 0.2 s.

In addition to 'fmincon', the results of GA have also been investigated and com-pared, as incorporated in Table XVI. It can be deduced that 'fmincon' has shorter total operating times in both island and grid connected modes. Additionally, compared to "GA", the deployment percentage with "fmincon" at which optimal solution is obtained is lower.

TABLE XVI
COMPARATIVE ANALYSIS OF FMINCON AND GA

	Islanded		Grid	
	Deploy-ment (%)	Total operating time (s)	Deploy-ment (%)	Total operating time (s)
Fmincon	0	98.9616	0	94.9524
	28.125	34.7971	33.33	32.7433
	100	23.5402	100	22.5934
GA	0	116.0846	0	102.56
	34.375	36.7971	39.394	34.26
	100	27.7564	100	25.48

V. CONCLUSION

This study proposes a novel approach that employs both conventional and dual-setting ROCOV relays and is applicable to both grid-connected and islanded operating modes. The protection coordination technique relies on analyzing the rate of voltage change to detect the fault and estimate the proper operation durations for all primary and backup relays in a meshed network. It can be inferred that:

1) The total operating times decrease for both islanded and grid-connected modes with the optimal number of DS-ROCOV relays.

2) Both standard and user-defined relay characteristics can be used to find the complete relay protection

scheme. However, user-defined characteristics provide a better solution than the standard one.

3) The proposed scheme is able to maintain the coordination between the primary and backup relays for different short circuit levels, i.e., during DG connection or disconnection whereas DS-DOCRs violate the C_{TI} limits in such situations.

4) In addition, the proposed scheme has been evaluated with various C_{TI} values, and it is found that regardless of the C_{TI} values, the optimal deployment (i.e., 28.125% for islanded and 33.33% for grid-connected) remains the same.

5) The simulation results show that the pro-posed approach can provide quick fault clearance through efficient and reliable coordination.

ACKNOWLEDGMENT

Not applicable.

AUTHORS' CONTRIBUTIONS

Praveen Kumar Gupta and Priyanshul Niranjan: problem formulation, simulation and calculations. Niraj Kumar Choudhary: problem conceptualization, execution and guidance. Nitin Singh and Ravindra Kumar Singh: problem conceptualization, and drafting the manuscript. All authors read and approved the final manuscript.

FUNDING

This work is carried out without the support of any funding agency.

AVAILABILITY OF DATA AND MATERIALS

Not applicable.

DECLARATIONS

Competing interests: The authors declare that they have no known competing financial interests or personal relationships that could have appeared to influence the work reported in this article.

AUTHORS' INFORMATION

Praveen Kumar Gupta has completed his M. Tech in electrical engineering from Motilal Nehru National Institute of Technology (MNNIT) Allahabad, Prayagraj (U.P), India. His areas of interest include power system analysis and power system protection.

Priyanshul Niranjan has completed his Ph.D. in electrical engineering from Motilal Nehru National Institute of Technology (MNNIT) Allahabad, Prayagraj (U.P), India. His areas of interest include power system analysis and power system protection.

Niraj Kumar Choudhary is presently working as an assistant professor in the Department of Electrical Engineering, MNNIT Allahabad, Prayagraj (U.P.), India. He has completed his Ph.D. in electrical engineering from MNNIT Allahabad. His research interest include renewable energy and distributed generation-based power system, power system protection, integration issues of DG in distribution system.

Nitin Singh is presently working as an associate Professor in the Department of Electrical Engineering, MNNIT Allahabad, Prayagraj (UP), India. He has completed his Ph.D. in electrical engineering from MNNIT Allahabad, India. His research interest includes power systems, artificial intelligence, and electrical machines.

Ravindra Kumar Singh is presently working as a professor (H.A.G) in the Department of Electrical Engineering, MNNIT Allahabad, Prayagraj (U.P.), India. He has completed his Ph.D. in electrical engineering from IIT Kanpur, India. His research interest include Power electronics, power system protection, and power systems.

REFERENCES

[1] M. Usama, H. Mokhlis, and M. Moghavvemi *et al*., "A comprehensive review on protection strategies to mitigate the impact of renewable energy sources on interconnected distribution networks," *IEEE Access*, vol. 9, pp. 35740-35765, Feb. 2021.

[2] N. Rezaei and M. N. Uddin, "An analytical review on state-of-the-art microgrid protective relaying and coordination techniques," *IEEE Transactions on Industry Applications*, vol. 57, no. 3, pp. 2258-2273, Feb. 2021.

[3] M. Singh, "Protection coordination in distribution systems with and without distributed energy resources- a review," *Protection and Control of Modern Power Systems*, vol. 2, no. 3, pp. 1-17, Jul. 2017.

[4] L. Huchel and H. H. Zeineldin, "Planning the coordination of directional overcurrent relays for distribution systems considering DG," *IEEE Transactions on Smart Grid*, vol. 7, no. 3, pp. 1642-1649, May 2016.

[5] C. J. Mozina, "Impact of smart grids and green power generation on distribution systems," in *2012 Rural Electric Power Conference*, WI, USA, May 2012, pp. C4-1-C4-13.

[6] N. Nimpitiwan, G. T. Heydt, and R. Ayyanar *et al.*, "Fault current contribution from synchronous machine and inverter based distributed generators," *IEEE Transactions on Power Delivery*, vol. 22, no. 1, pp. 634-641, Jan. 2007.

[7] M. Singh, B. K. Panigrahi and A. R. Abhyankar, "Optimal coordination of directional over-current relays using teaching learning-based optimization (TLBO) algorithm," *International Journal of Electrical Power & Energy Systems*, vol. 50, pp. 33-41, Sept. 2013.

[8] E. Dehghanpour, H. Kazemi Karegar, and R. Kheirollahi *et al.*, "Optimal coordination of directional overcurrent

relays in microgrids by using cuckoo-linear optimization algorithm and fault current limiter," *IEEE Transactions on Smart Grid*, vol. 9, no. 2, pp. 1365-1375, Mar. 2018.

[9] C. A. C. Salazar, A. C. Enríquez, and S. E. Schaeffer, "Directional overcurrent relay coordination considering non-standardized time curves," *Electric Power Systems Research*, vol. 122, pp. 42-49, May 2015.

[10] K. Chheng, A. Priyadi, and M. Pujiantara *et al.*, "The coordination of dual setting DOCR for ring system using adaptive modified firefly algorithm," in *2020 International Seminar on Intelligent Technology and Its Applications (ISITIA)*, Surabaya, Indonesia, Aug. 2020, pp. 44-50.

[11] A. Srivastava, J. M. Tripathi, and R. Krishan *et al.*, "Optimal coordination of overcurrent relays using gravitational search algorithm with DG penetration," *IEEE Transactions on Industry Applications*, vol. 54, no. 2, pp. 1155-1165, Mar. 2018.

[12] A. Sharma, D. Kiran, and B. K. Panigrahi, "Planning the coordination of overcurrent relays for distribution systems considering network reconfguration and load restoration," *IET Generation Transmission and Distribution*, vol. 12, no. 7, pp. 1672-1679, Feb. 2018.

[13] R. Tiwari, R. K. Singh, and N. K. Choudhary, "Coordination of dual setting overcurrent relays in microgrid with optimally determined relay characteristics for dual operating modes," *Protection and Control of Modern Power Systems*, vol. 7, no. 1, pp. 1-18, Jan. 2022.

[14] A. Srivastava, J. M. Tripathi, and S. R. Mohanty *et al.*, "Optimal over-current relay coordination with distributed generation using hybrid particle swarm optimization-gravitational search algorithm," *Electric Power Systems Research*, vol. 44, no. 5, pp. 506-517, Mar. 2016.

[15] J. Radosavljević and M. Jevtić, "Hybrid GSA-SQP algorithm for optimal coordination of directional overcurrent relays", *IET Generation Transmission and Distribution*, vol. 10, no. 8, pp. 1928-1937, May 2016.

[16] H. M. Sharaf, H. H. Zeineldin, and D. K. Ibrahim *et al.*, "A proposed coordination strategy for meshed distribution systems with DG considering user-defned characteristics of directional inverse time overcurrent relays," *International Journal of Electrical Power and Energy Systems*, vol. 65, pp. 49-58, Feb. 2015.

[17] R. Tiwari, R. K. Singh, and N. Kumar Choudhary, "Optimal coordination of dual setting directional over current relays in microgrid with different standard relay characteristics," in *2020 IEEE 9th Power India International Conference (PIICON)*, Sonepat, India, Jun. 2020, pp. 1-6.

[18] H. Beder, B. Mohandes, and M. S. E. Moursier *et al.*, "A new communication-free dual setting protection coordination of microgrid," *IEEE Transactions on Power Delivery*, vol. 36, no. 4, pp. 2446-2458, Aug. 2021.

[19] H. H. Zeineldin, H. M. Sharaf, and D. K. Ibrahim *et al.*, "Optimal protection coordination for meshed distribution systems with DG using dual setting directional over-current relays," *IEEE Transactions on Smart Grid*, vol. 6, no. 1, pp. 115-123, Jan. 2015.

[20] H. M. Sharaf, H. H. Zeineldin, and E. El-Saadany, "Protection coordination for microgrids with grid-connected and islanded capabilities using communication assisted dual setting directional overcurrent relays," *IEEE Transactions on Smart Grid*, vol. 9, no. 1, pp. 143-151, Jan. 2018.

[21] A. Yazdaninejadi, D. Nazarpour, and S. Golshannavaz, "Dual-setting directional over-current relays: an optimal coordination in multiple source meshed distribution networks," *International Journal of Electrical Power & Energy Systems*, vol. 86, pp. 163-176, Mar. 2017.

[22] V. C. Nikolaidis, E. Papanikolaou, and A. S. Safigianni, "A communication-assisted overcurrent protection scheme for radial distribution systems with distributed generation," *IEEE Transactions on Smart Grid*, vol. 7, no. 1, pp. 114-123, Jan. 2016.

[23] A. Yazdaninejadi, S. Golshannavaz, and D. Nazarpour *et al.*, "Dual-setting directional overcurrent relays for protecting automated distribution networks," *IEEE Transactions on Industrial Informatics*, vol. 15, no. 2, pp. 730-740, Feb. 2019.

[24] K. A. Saleh, H. H. Zeineldin, and Al-Hinai *et al.*, "Dual-setting characteristic for directional overcurrent relays considering multiple fault locations," *IET Generation Transmission and Distribution*, vol. 99, no. 12, pp. 1332-1340, Sept. 2015.

[25] S. Jamali and H. Borhani-Bahabadi, "Protection method for radial distribution systems with DG using local voltage measurements," *IEEE Transactions on Power Delivery*, vol. 34, no. 2, pp. 651-660, Apr. 2019.

[26] L. Hong, M. Rizwan, and M. Wasif *et al.*, "User-defined dual setting directional overcurrent relays with hybrid time current-voltage characteristics-based protection coordination for active distribution network," *IEEE Access*, vol. 9, pp. 62752-62769, Apr. 2021.

[27] A. A. Balyith, H. M. Sharaf, and M. Shaaban *et al.*, "Non-communication based time-current-voltage dual setting directional overcurrent protection for radial distribution systems with DG," *IEEE Access*, vol. 8, pp. 190572-190581, Oct. 2020.

[28] S. Dadfar and M. Gandomkar, "Augmenting protection coordination index in interconnected distribution electrical grids: optimal dual characteristic using numerical relays," *International Journal of Electrical Power & Energy Systems*, vol. 131, Oct. 2021.

[29] S. K. Salman, D. J. King, and G. Weller, "New loss of mains detection algorithm for embedded generation using rate of change of voltage and changes in power factors," in *2001 Seventh International Conference on Developments in Power System Protection (IEE)*, Amsterdam, Netherlands, Aug. 2001, pp. 82-85.

[30] A. Rostami, A. Jalilian, and M. T. Hagh *et al*. "Islanding detection of distributed generation based on rate of change of exciter voltage with circuit Breaker Switching Strategy," *IEEE Transactions on Industry Applications*, vol. 55, no. 1, pp. 954-963, Jan. 2019.

[31] A. Rostami, H. Abdi, and M. Moradi *et al.*, "Islanding detection based on ROCOV and ROCORP parameters in the presence of synchronous DG applying the capacitor connection strategy," *Electric Power Components and Systems*, vol. 45, no. 3, pp. 230-315, Dec. 2017.

[32] M. N. Alam, "Adaptive protection coordination scheme using numerical directional overcurrent relays," *IEEE*

Transactions on Industrial Informatics, vol. 15, no. 1, pp. 64-73, Jan. 2019.

[33] M. A. Dawoud, D. K. Ibrahim, and M. I. Gilany *et al.*, "Robust coordination sheme for microgrids protection based on the rate of change of voltage," *IEEE Access*, vol. 9, pp. 156283-156296, Nov. 2021.

[34] M. A. Dawoud, D. K. Ibrahim, and M. I. Gilany *et al*., "Proposed application for rate of change of phasor voltage in fault detection and coordination studies in MV distribution networks," *Iranian Journal of Science and Technology, Transactions of Electrical Engineering*, vol. 45, no. 3, pp. 815-831, Sept. 2021.

[35] S. Agrawal, B. K. Panigrahi, and M. K. Tiwari, "Multiobjective particle swarm algorithm with Fuzzy clustering for electrical power dispatch," *IEEE Transactions on Evolutionary Computation*, vol. 12, no. 5, pp. 529-541, Oct. 2008.

[36] Z. Bo and C. Yi-jia, "Multiple objective particle swarm optimization technique for economic load dispatch," *Journal of Zhejiang University*, vol. 6, no. 5, pp. 420-427, May 2005.